Chapter 11

Amplification and Filtering in Biomedical Applications

11.1 Introduction

There has been a lot of development in the use of biomedical equipment for diagnostic and treatment purposes in recent times. A good amount of literature has come from the interdisciplinary area of medical engineering, medical instrumentation, and so on, making medical electronics a specialized field of study. An important constituent of electronics engineering is the study of analog filters. Hence, the design and application of analog filters finds a place in the books and literature on medical engineering and medical instrumentation too. The design of analog filters especially the continuous-time types requires special attention. However, the available books on analog filter design do not adequately relate filter design with biomedical applications. A few simple examples included in this chapter will try to bridge the gap between theoretical design and the application of analog filters in this important field.

We have already studied the basics of continuous-time analog filter in the previous chapters. In this chapter, we will first connect the design of a filter to its utilization in the field of biomedical electronics.

It is a well-known fact that cells in the human body have different element (Na^+, K^+, Ca^{++}, Cl^-) ion concentrations inside and outside the membrane. This difference in ion concentration creates a small electric potential called *biopotential*. When there is a disturbance in a biopotential, an *action potential* is generated which is the result of depolarization and repolarization of the cells in the human body. It is the action potential at the location (nodes) on the body which is detectable and can be processed using biomedical circuits. When such signals generated by the heart are collected, it makes up the electrocardiogram (ECG). ECG detectors use electrodes to collect these signals, which are amplified, filtered and displayed for data analysis. ECG signals

https://doi.org/10.1017/9781108762632.012 Published online by Cambridge University Press

require filtering and amplification to produce high-quality signals. Not only are different stages of amplification used, specific signal processing is also required. Therefore, instead of a simple (DA) differential amplifier, instrumentation amplifiers (inst-amp) are used. Section 11.2 discusses the the necessity of converting DA into an inst-amp. Transformation of the inst-amp into a biopotential amplifier and as integrated circuit inst-amps especially suitable in medical instruments and devices are discussed in Section 11.3 along with a case study on a piezoelectric transducer.

A brief description of the characteristics of physiological signals is included in Section 11.4. Analog front-ends (AFEs) used in ECG detection is considered in Section 11.5, which shows that amplification and analog filtering are essentials. As an example, an AFE system using an on-chip filter is also discussed.

It is rightly assumed that signals from the heart are important. However, signals from other body parts also play an important role in diagnostics. The rest of the chapter discusses a few such cases. Utilization of inst-amp and filters for collecting electromyographic (EMG) signals is shown in Section 11.6. Filtering in brain–computer interface applications and chamber plethysmography is briefly discussed in Sections 11.8 and 11.9. The chapter concludes with the application of an eighth-order filter for simulating the frequency response of a human ear.

11.2 Instrumentation Amplifiers

Figure 11.1 shows a conventional simple differential amplifier (DA) using a single OA. In the circuit, the following resistance relation exists:

$$R_1 = R_3 \text{ and } R_2 = R_4 \tag{11.1}$$

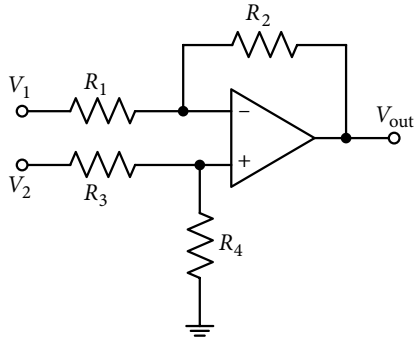

Figure 11.1 Commonly used differential amplifier circuit.

Then considering OA as ideal, the voltage gain of the DA is obtained as:

$$\frac{V_{out}}{V_{in}} = \frac{V_{out}}{V_2 - V_1} = \frac{R_2}{R_1} = \frac{R_4}{R_3} \tag{11.2}$$

https://doi.org/10.1017/9781108762632.012 Published online by Cambridge University Press

The circuit is very useful and functions well as an inst-amp, which amplifies the differential signal $V_{in} = (V_2 - V_1)$ and rejects the common mode signal. However, as application requirements become strict, limitations of the circuit become obvious. For instance, input impedances at the inverting and non-inverting terminals are not very high; they are also unequal. Hence, if the signal is applied to only one terminal and the other terminal remains grounded, different currents flow in the two terminals; it degrades the common mode rejection ratio (CMRR).

In addition, the circuit requires a very close resistance ratio matching of equation (11.1). Even a small mismatch in the resistance ratios degrades the CMRR. This degraded value of CMRR may not be acceptable in many practical applications like precision instrumentation and especially in medical applications.

11.3 Differential Biopotential Amplifier

Figure 11.2 shows a simple differential biopotential amplifier. When bio-electrodes are placed on a body, electro-physical actions generate a potential difference across them. The first stage of the pre-amplifier rejects the changes in the common mode signals detected simultaneously by both the bio-electrodes. The pre-amplifier comprises OA1 as a DA, for which low frequency gain $\frac{R_3}{R_2} = \frac{R_4}{R_1}$ is generally the gain which is set at nearly 1000. However, with such a high gain, the pre-amplifier will work only when the dc offset is limited to 10 mV; otherwise, the OA will saturate. To use the circuit as part of the surface ECG amplifier, the design value of the gain is to be considerably reduced because offset may go even up to 300 mV [11.1].

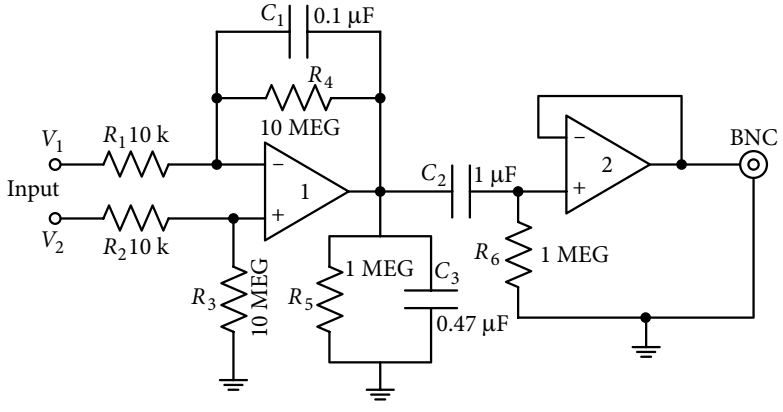

Figure 11.2 A simple differential bio-potential amplifier.

As capacitor C_1 offers low impedance at higher frequencies, resistance R_4 becomes ineffective and the first stage, using OA1, acts as a low pass filter (LPF). It also limits the bandwidth (3 dB frequency ≈ 160 Hz) of the amplifier eliminating high frequency noise. Capacitors C_1 and

https://doi.org/10.1017/9781108762632.012 Published online by Cambridge University Press

C_3, which act as a bypass, clamp oscillation and reduce instabilities in the circuit. Capacitor C_2 along with R_6 acts as a high pass filter (HPF) (3 dB frequency ≈ 0.16 Hz), and the unity gain follower OA2 acts as signal buffer.

The circuit has also been found very useful in measuring the CMR and input impedance of a biopotential amplifier [11.1].

3 OA Instrumentation Amplifier- A simple and obvious method for improving the performance of the DA shown in Figure 11.1 is through the addition of high impedance buffer amplifiers. This arrangement works well up to a certain level of accuracy; hence, further improvements are made by operating the buffers with gain providing additional flexibility. Such an improved form of the circuit is shown in Figure 11.3; it is popularly known as an *instrumentation amplifier*.

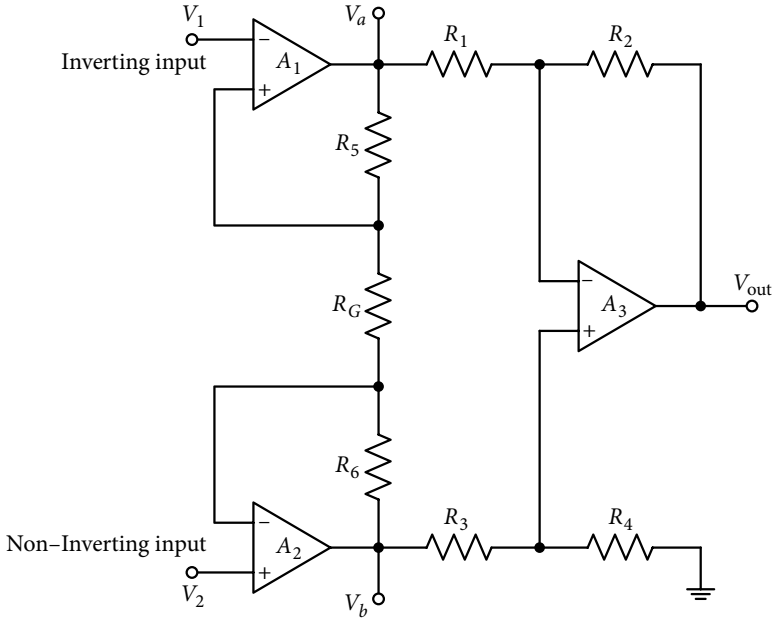

Figure 11.3 The classic 3OA instrumentation amplifier circuit.

Input OA1 and OA2 can be analyzed as non-inverting amplifiers. Therefore, applying superposition, output voltages V_a and V_b are found as:

$$V_a = \left(1 + \frac{R_5}{R_G}\right)V_1 - \left(\frac{R_5}{R_G}\right)V_2 \tag{11.3}$$

$$V_b = \left(1 + \frac{R_6}{R_G}\right)V_2 - \left(\frac{R_6}{R_G}\right)V_1 \tag{11.4}$$

https://doi.org/10.1017/9781108762632.012 Published online by Cambridge University Press

With resistance equality of equation (11.1) satisfied, the gain of the DA OA3 is (R_2/R_1). Hence, the expression of the output voltage with $R_5 = R_6$ will become:

$$V_{\text{out}} = (V_b - V_a)(R_2/R_1) = (V_2 - V_1)(1 + 2R_5/R_G) \tag{11.5}$$

Therefore, the gain of the amplifier is $(1 + 2R_5/R_G)$ which is controllable with a single resistor R_G.

11.3.1 Integrated circuit monolithic instrumentation amplifier

In practice, bio-potential amplifiers are hardly built now in terms of individual OAs. Instead, all the components are integrated on a single chip to constitute an inst-amp, called an integrated circuit instrumentation amplifier (ICIA) or a monolithic instrumentation amplifier.

Monolithic IC inst-amp are mostly based on variations of 2OAs and 3OAs DA circuits and resistors are mostly laser-trimmed for improved accuracy. Additionally, both active and passive components are closely matched being on the same chip and placed very close to each other; which is an essential requirement of the circuit. It helps in getting high CMR. An additional advantage of a monolithic inst-amp is that they are easy to use as they are available in various packages like very small, very low-cost SOIC, MSOP or LFCSP (chip scales) packages. A good discussion on a large number of monolithic inst-amps is available in *Analog Devices* [11.2]. A large number of monolithic inst-amps are being manufactured for general and specific applications [11.3].

One of the commonly used ICIA is INA 102 from Burr Brown Corporation [11.4]. The INA 102 is a high-accuracy monolithic inst-amp designed for signal conditioning applications where low quiescent power is required. Its prominent features are: low quiescent current of 750 μA max, internal gains of 1, 10, 100 and 1000, high CMR of 90 dB min, low offset voltage of 100 μV max and high input impedance of $10^{10}\,\Omega$.

To illustrate the working of an inst-amp, a brief discussion and design steps of a specific case is presented here [11.5]. It is expected that the procedure can equally be applied to similar cases, being typical in nature.

A Case Study: A piezoelectric transducer produces signals which are conditioned and fed to a 250 kc/s, 12-bit ADC (analog to digital convertor) with an input voltage range of 0-5V. Maximum amplitude of the differential voltage from the sensor is expected to be 20 mV. Bandwidth of the sensor is not known but the presumed high frequency range needs to be band limited so as not to saturate the next stage inst-amp.

Based on the input signal magnitude, the frequency range, and the ADC to be employed, signal conditioning specifications are found and implemented using a chain of circuits. However, our focus being on analog filters, only that part will be highlighted here.

A pass band of 50 kHz was selected for an LPF, considering that almost all the relevant information from the transducer is expected to be contained in this frequency range. Permissible

https://doi.org/10.1017/9781108762632.012 Published online by Cambridge University Press

variation in amplitude was taken as 5%. This figure of 5% comes from the data sheet of the transducer, as it is calibrated within 5% of the actual value in the selected frequency pass band. A maximum of 5% non-linearity in phase was taken as a rule of thumb [11.6].

The signal conditioning arrangement is shown in Figure 11.4 in block form. The signal produced by the transducer is buffered and amplified by an inst-amp. It is then amplified to a level compatible with full ADC resolution. A LPF band limits the signal before it reaches the ADC. Data retrieved from memory is then un-inverted and further processed.

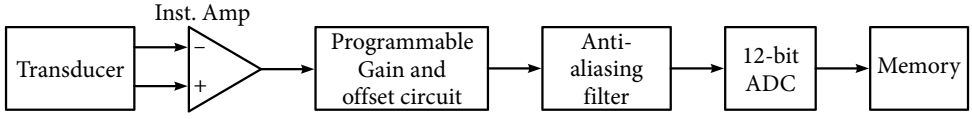

Figure 11.4 Signal conditioning sequence for a piezoelectric transducer signal [11.5].

A piezoresistive transducer is used with a Wheatstone's bridge built into the transducer packing. Output of the transducer circuit is a differential signal with an expected maximum amplitude of 20 mV.

A differential inst-amp is used to provide high-impedance buffering; it attenuates unwanted common-mode noise in the signal from the transducer. However, prior to the inst-amp, a first-order passive filter reduces undesired high-frequency signals. The first-order filter also forms the first pole of the seven poles of the anti-aliasing filter to be used before ADC.

In the present application, the inst-amp is required to have high DC precision, low noise, high CMRR and high input impedance. The AD8224B inst-amp shown in Figure 11.5(a) is selected because it can satisfy the aforementioned requirements. Its slew rate being 2 V/μs and with a maximum output of 100 mV (p-p for its gain of 5), full-power bandwidth (FPBW) is calculated using equation (11.6):

$$\text{FPBW} = \frac{\text{SR}}{2\pi V_{p-p}} = \frac{2\times10^6}{2\pi\times0.1} = 3.18\,\text{MHz} \tag{11.6}$$

The calculated value of the FPBW shows that the slew rate limitation will not affect the inst-amp. Figure 11.5(b) shows the simulated response of the inst-ampl of Figure 11.5(a) with a voltage gain of 4.985 {$(1 + 49.4/R_g)$ and R_g = 12.4 kOhm} and a 3-dB frequency of 59.1 kHz (1/150 pF × 2 × 8.87 k = 375.8 krad/s).

While using the inst-amp, it is important to consider the output load of the transducer, which is approximately (650±350) Ω. Obviously, this load will modify the 3-dB frequency of the passive filter.

Output of the inst-amp is passed on to a programmable gain circuit and voltage offset circuit. These circuits allow the system to bring the signal within the full scale range of the ADC [11.5].

https://doi.org/10.1017/9781108762632.012 Published online by Cambridge University Press

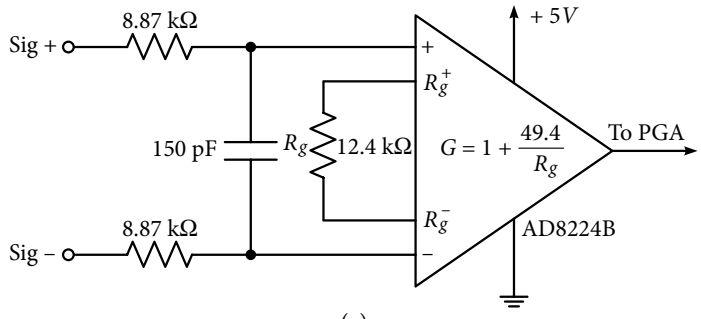

(a)

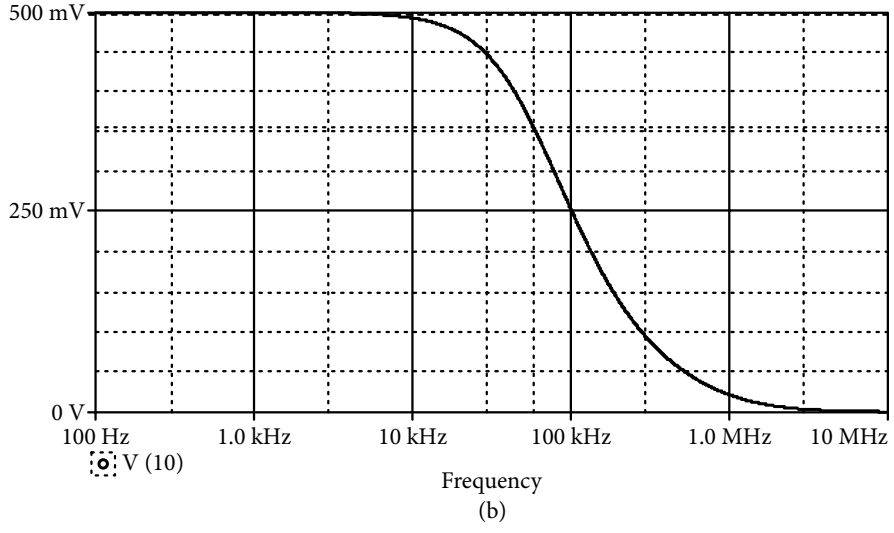

(b)

Figure 11.5 (a) The AD8224B instrumentation amplifier [11.5]. (b) Simulated magnitude response of the instrumentation amplifier shown in Figure 11.5(a).

Low Pass Anti-aliasing Filter: An ADC requires 6 dB of attenuation per bit at the Nyquist frequency [11.8]. Hence, a 12-bit ADC requires 72 dBs attenuation This means that if aliasing is allowed in the transition region (from 50 kHz to the sampling frequency of 250 kHz), 72 dBs attenuation is to be achieved at the sampling frequency (250 kHz) minus the highest non-aliased frequency (50 kHz), that is 200 kHz. For these specifications in terms of attenuation, the order of the filter can be calculated using the steps described in Chapter 3. Of course, the filter will depend on the type of the magnitude approximation used. In this case, Butterworth approximation was preferred and the following relation was used to find its order [11.8].

$$N \geq \frac{3 \times \text{Bits}}{10\log\left(f_s / f_c\right)} = \frac{3 \times 12}{10\log\left(250\,\text{kHz} / 50\,\text{kHz}\right)} \geq 6 \tag{11.7}$$

https://doi.org/10.1017/9781108762632.012 Published online by Cambridge University Press

Here, $f_s = 250$kHz is the sampling frequency and $f_c = 50$kHz is the pass band frequency; the required order of the Butterworth filter is seven. One of the choices for realizing a seventh-order filter is to apply the cascade approach. Hence, from Table 3.1, location of the poles for the seventh-oder filter is obtained as:

$$s_{1,2} = -0.9009 \pm j0.4338,\ s_{3,4} = -0.2225 \pm j0.9649$$

$$s_{5,6} = -0.6234 \pm j0.7818,\ s_7 = -1.0 \tag{11.8}$$

Out of the seven poles in equation (11.8), the real pole s_7 was already realized prior to the inst-amp. The remaining six poles are to be realized using three second-order LP sections. Many choices are available for realizing second-order sections. However, after comparison between the Sallen and Key circuit (Section 7.7) and the multiple feedback (MF) topology (Section 7.3), the latter was selected in the report. The free Texas Instrument Filter Pro Desktop tool was used to design the three filter sections [11.7]. The sections were ordered in increasing value of pole-Q as described in Section 10.3.2. As input to the filter was limited to 4 V, the gain of the first two sections was unity and for the last section, gain was 1.25 to provide full 5 V to the ADC. The OA OP462 was employed as it has a slew rate of 10 V/μs for a maximum peak-to-peak voltage of 5 V.

Figure 11.6(a) shows the cascade arrangement in block form. The three second-order sections use the MF LP circuit of Figure 7.6 with the following respective element values; the corner frequency for the sections was 60 kHz.

$$R_{11} = 24\ \text{k}\Omega,\ R_{31} = 12\ \text{k}\Omega,\ R_{41} = 24\ \text{k}\Omega,\ C_{21} = 240\ \text{pF},\ C_{51} = 100\ \text{pF}$$

$$R_{12} = 16.5\ \text{k}\Omega,\ R_{32} = 8.25\ \text{k}\Omega,\ R_{42} = 16.5\ \text{k}\Omega,\ C_{22} = 510\ \text{pF},\ C_{52} = 100\ \text{pF}$$

$$R_{13} = 4.7\ \text{k}\Omega,\ R_{33} = 2.61\ \text{k}\Omega,\ R_{43} = 5.9\ \text{k}\Omega,\ C_{23} = 4.7\ \text{nF},\ C_{53} = 100\ \text{pF} \tag{11.9}$$

In addition, resistances of 24 kΩ, 16.5 kΩ and 5.23 kΩ were connected at the non-inverting terminals of the respective three sections to equalize input bias currents in the OAs.

The simulated response of the three sections combined with the first-order section (and gain of 5 for the inst-amp) is shown in Figure 11.6(b). The overall gain is 6.274 with a 3-dB frequency of 59.59 kHz. At 200 kHz, attenuation from the pass band is 73.55 dBs, which satisfies the specifications.

11.4 Physiological Signals

Signals resulting from physiological activities can be considered as a communication system transmitting information from one part of the body to another. We can detect these signals from those parts of the body where many neurons activate simultaneously to create a single

https://doi.org/10.1017/9781108762632.012 Published online by Cambridge University Press

event. Accurate detection of these signals is very important as their interpretation can indicate whether a body part is healthy or not. Due to their low amplitude and the method of observing/detecting these signals from the body parts, they are processed using *biopotential amplifiers*. These amplifiers have high gain in the range of 1000 or more and some specific characteristics that will be described here in brief.

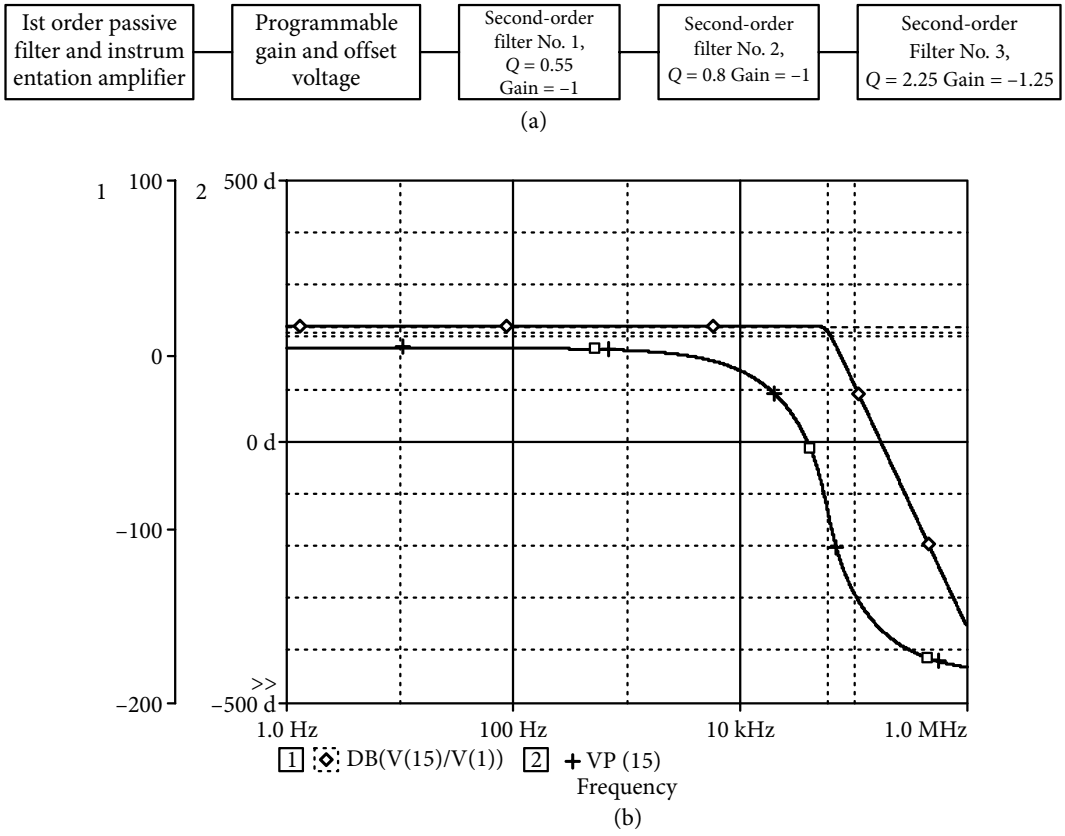

Figure 11.6 (a) Cascade arrangement in block form for filtering and amplification of signals from a piezoelectric transducer: a case study [11.5]. (b) Simulated magnitude and phase response of the seventh-order low pass filter for Figure 11.6(a), employing elements as given in equation (11.9).

Like any other amplifier, the bandwidth requirement of the biopotential amplifier depends on the frequencies present in the physiological signals of interest, which are sometimes in the range of a fraction of Hz to a few Hz or from a few Hz to a few kHz.

A number of noise signals corrupt the basic signal, like those due to magnetic induction in wires, equipment interconnections and imperfections. Noise signals are also generated due to the displacement current in the electrode leads and in the body. Another significant noise factor is due to the changing magnetic field of the AC power supply; this is at a rate of 50 Hz/60Hz and caused by induction. The changing magnetic field causes alternating current

https://doi.org/10.1017/9781108762632.012 Published online by Cambridge University Press

to flow to ground through the signal measurement system. All these noise signals are to be attenuated heavily.

A likely error may occur due to common-mode signals. Therefore, a very high value of common mode rejection ratio (CMRR) is required. Otherwise, even a small common-mode voltage gets amplified because of the large amplifier gain of the device used, which may saturate active components, causing great errors.

Physiological signals are collected using metal electrodes which are in contact with the body through an electrolyte. This process results in a voltage known as *half-cell potential*. This DC potential must be taken care of by the amplifier; otherwise, it will also saturate active components.

Most biopotential amplifiers are OA based. Single-ended OA base amplifiers were used in the past in the front-end stage. However, with the availability of low-cost integrated instrumentation amplifiers (IIA), single-ended and conventional DAs have been replaced. There are a number of IIAs available for general and specific applications from world class manufacturers [11.9].

11.5 Analog Front-end for ECG Signal

As mentioned in the previous section, electrical signals may be detected from a human body part. One of the most important signals comes from heart muscles. The measurement of these signals and their graphic representation are known as electrocardiogram (ECG or EKG). The basics of ECG measurements are almost the same for any type of application, for example, whether it is monitoring of heart rate that is required or diagnosis of any heart condition, or signals are obtained from any other part of the body. However, the electrical components and their specifications vary substantially depending upon application and usage.

All ECG signals (heart signals) collected through electrodes which are located at different parts of the body have amplitudes of a few mV. These signals are processed and finally displayed as a channel on the ECG print out. There is more than one channel for ECG monitoring; they are referred to as *leads*. For example, a 12-lead ECG device has 12 separate channels. The required electronic components for an ECG can be separated into the analog front-end (AFE) and the *rest of the system* [11.10]. Though AFEs are fundamentally similar, they differ in terms of the number of leads, fidelity of signal, nature and magnitude of noises, and so on. The primary function of the AFE is to digitize the heart signals for processing, which is then again converted as a function of time for display. The architecture of an AFE may have a *brute force* type which provides high fidelity over a wide frequency range or a *minimal AFE*, a consumer-grade ECG. Circuits in most ECG devices lie between the two extremes of brute force type or of minimal type.

When IC inst-amp (IIA) is used for amplification of small input signals, common-mode voltage rejection and elimination of noise also takes place. IIA also provides a buffer for the sampling capacitances of the ADC. Filters before and after the IIA remove noise and band limits the incoming signals. Without going into any further detail of the ECG system, let us take some practical examples of the application of analog filters in the medical field.

https://doi.org/10.1017/9781108762632.012 Published online by Cambridge University Press

11.5.1 An AFE system with low power on-chip filter

Different types of ECG equipment include telemetry devices, Holter monitors, consumer ECGs and diagnostic ECGs. Diagnostic ECGs are used in hospitals and doctors' offices to perform high-quality ECG tests. For reasons of portability and durability of ECG equipment, an attempt is made to reduce the power consumption. In line with this requirement, the basic parts of a portable AFE system are shown in Figure 11.7(a). Here, the *acquisition board* converts the body signals to six leads. The acquisition board consists of an inst-amp, an HPF, a (50 Hz/60 Hz) notch filter and a common-level-adjuster [11.11]. Amplitude of the ECG signal is in the range of 100 μV to 4 mV [11.12]. With such a low level of signal, it is required that a signal-to-noise and distortion ratio (SNDR) must be at least 32 dBs (that is, 6 bits). The next important specification is that of the frequency range of useful ECG signals, which lies between 0.1 Hz and 250 Hz. Hence, the on-board analog LPF is designed for its 3-dB frequency of 250 Hz, and an HPF with a 3-dB frequency of 0.1 Hz is used to attenuate noise below 0.1 Hz. The active RC HPF structure shown in Figure 11.7(b) was used. The following element values are obtained employing design equations (7.69)–(7.70):

$R_1 = 483\ \text{k}\Omega$, $R_2 = R_3 = R_4 = 100\ \text{k}\Omega$, and $C_1 = C_2 = 15.9\ \mu\text{F}$

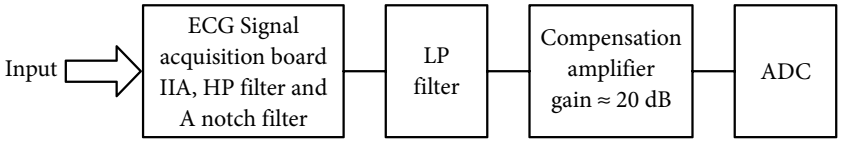

(a)

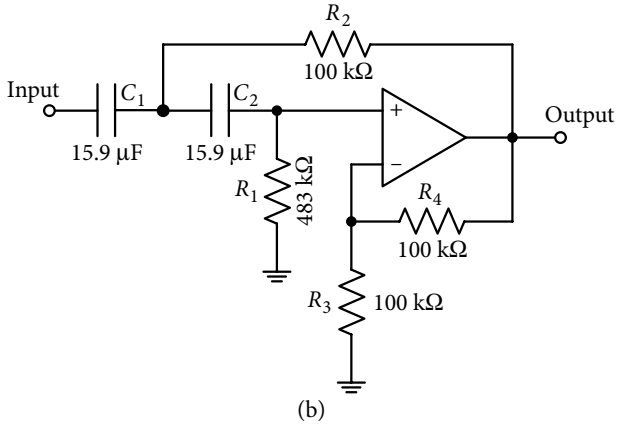

(b)

https://doi.org/10.1017/9781108762632.012 Published online by Cambridge University Press

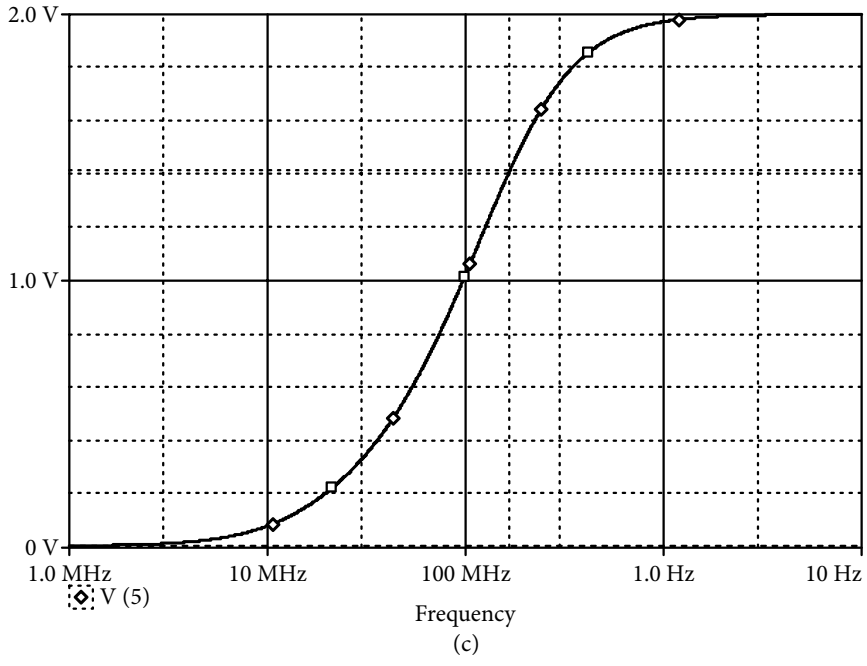

Figure 11.7 (a) An *analog front-end* system for portable EGC detection device [11.11]. (b) Second-order Sallen–Key high pass filter. (c) Simulated response of the high pass filter shown in Figure 11.7(b).

Using the 741 OA, its PSpice simulated response is shown in Figure 11.7(c). Its cut-off frequency is 0.167 Hz and high frequency gain is 2 as $R_3 = R_4$.

The last stage on the acquisition board is a notch filter using a twin-tee based active RC circuit shown in Figure 11.8(a) to attenuate the power supply noise frequency of 50 Hz/60 Hz. Its simulated response is shown in Figure 11.8(b). For a notch frequency of 60 Hz, $R =$ 530 kΩ and $C = 5$ nF and for a notch frequency of 50 Hz, $R = 470$ kΩ and $C = 6.798$ nF.

Switched capacitor filters have been recommended for long-term physical detection and monitor systems [11.13]. However, power consumption in OAs increase due to leakage when the sampling frequency is low in the kHz range. It is for this reason that continuous-time operational transconductance amplifier (OTA) based filters are preferred for low frequency operation. For further reduction in power consumption, OTAs are to be used in sub-threshold regions with ultra-low transconductance [11.14].

As mentioned earlier, an anti-aliasing filter is to be used to attenuate the out-of-band interference before the ADC. A fifth-order ladder type Butterworth filter selected for its realization in OTA-C form is used. The advantage of a ladder structure have been discussed previously. OTA base fifth-order Butterworth filters with a designed 3-dB frequency of 250 Hz will be shown in Chapter 15.

https://doi.org/10.1017/9781108762632.012 Published online by Cambridge University Press

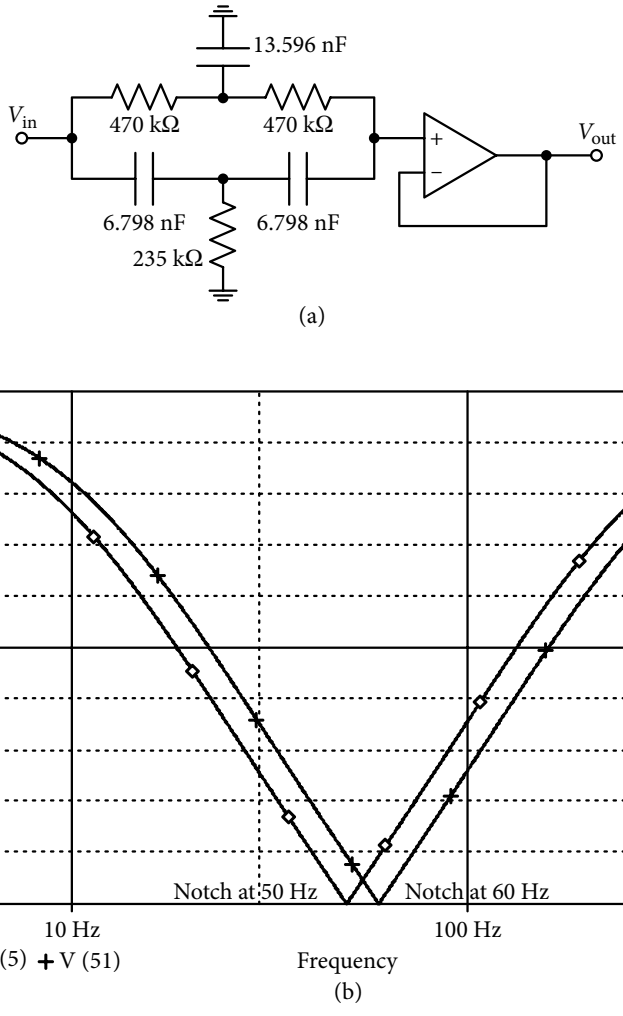

Figure 11.8 (a) Twin-T based notch filter circuit (notch at 50 Hz). (b) Response of the notch filter shown in Figure 11.8(b) at 50 and 60 Hz.

Why continuous-time analog filters, especially using OTAs are preferable over switched capacitor filters for low frequency medical applications is emphasized in another publication [11.15]. A 2.4 Hz sixth-order Bessel LP filter achieving 60-dB dynamic range was fabricated in 0.8 μm CMOS technology to illustrate the usefulness of continuous-time analog filters.

11.5.2 ECG signal acquisition system: an application example

A real-time ECG signal acquisition system has been introduced with DSP chip TMS320VC5509A at its core [11.16].

https://doi.org/10.1017/9781108762632.012 Published online by Cambridge University Press

It has been mentioned before that ECG signals are bipolar, low frequency, low amplitude signals having an amplitude ranging from 10 μvolts to 4 milli volts. The frequency ranges in between 0.05 Hz and 100 Hz, but is mostly concentrated in 0.05–35 Hz. Because of the low level of the signals, they need to be analog filtered and amplified. In almost all cases, a preamplification is done using an inst-amp. After pre-amplification, a BPF (band pass filter) circuit employing OA OPA 2604 is used. It is a combination of an HPF and an LPF having corner frequencies of 0.05 Hz and 100 Hz, respectively. The circuit structure is shown in Figure 11.9(a). A combination of capacitors of 47 μF and 68 kΩ resistors work as HPF and a combination of 1 μF capacitors with 1.6 kΩ resistors provide LP response. The simulated response of the combined LP and the HP filters in Figure 11.9(b) shows its BP characteristics.

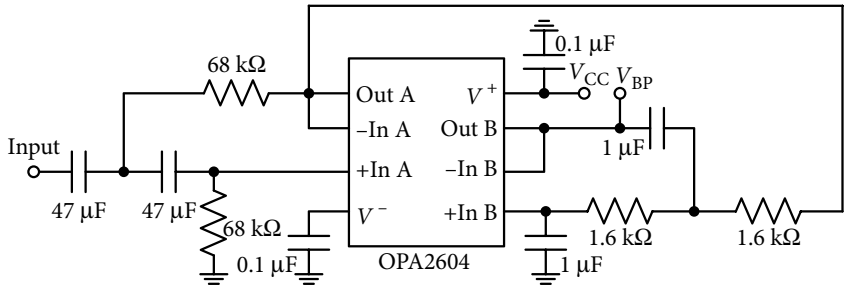

(a)

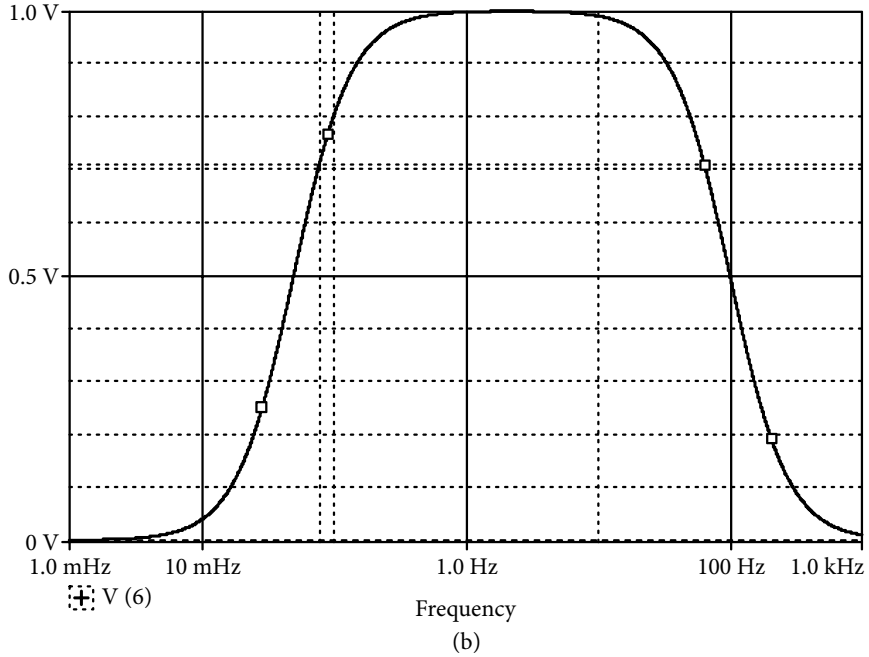

(b)

Figure 11.9 (a) Combination of high pass and low pass filters using OPA 2604 and [11.16]; {with permission from J Wang, et al} (b) its combined simulated response.

https://doi.org/10.1017/9781108762632.012 Published online by Cambridge University Press

11.6 Filtering of Surface Electromyography Signals

Electromyography (EMG) relates to the study of electrical signals transmitted by body muscles, similar to the way nerves transmit signals. These electrical signals give rise to *muscle action potential*. Surface EMG is a method of collecting and recording the information present in these muscle action potentials.

The idea of having myoelectric control of the movement of artificial limbs, say hand, using EMG signals is sufficiently old. Great progress has occurred and collecting EMG signals from the human body is now a routine procedure, both in rehabilitation and in medical research. EMG signals are very weak, within a range of few μVolts to low milli volts (0-6 mV_{pp}), and they contain noise signals due to different reasons. The frequency range of the useful EMG signal is mostly in the 0-500 Hz range, whereas the dominant component lies in the 50–150 Hz range.

Because of the very small magnitude of the EMG, it needs amplification of the order of 1000 to 10,000, while keeping in mind that noise is to be minimized and not amplified during signal amplification. Figure 11.10 shows an arrangement in block form of amplification and noise elimination through filtering. Obviously, HP and LP filtering form important components of the process before the EMG signal is fed into an ADC [11.17].

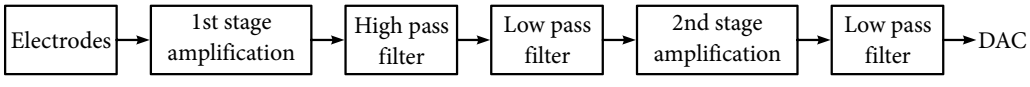

Figure 11.10 Block diagram of amplification and filtering for electromyographic signals. {With permission from Wang et al.[11.17]}.

The preamplifier consists of an inst-amp INA 128 and an OA OPA 2604. In this case, the gain of the preamplifier was set at around 10 and a Sallen–Key second-order HPF having a corner frequency of 20 Hz was used. The circuit structure and element values are shown in Figure 11.11(a). Expressions for the corner frequency and pass band gain are:

$$f_c = 1/2\pi\sqrt{(R_1R_2C_1C_2)},\ \text{Gain} = 1 + R_4/R_5 \tag{11.10}$$

For obtaining a fourth-order HPF with the same corner frequency, two sections of Figure 11.11(a) were connected in cascade. However, the element values for each of the two sections are given as follows for the corner frequency of 20 Hz:

$$R_1 = R_2 = 560\ \text{k}\Omega,\ R_3 = 51\ \text{k}\Omega,\ R_4 = 16\ \text{k}\Omega,\ C_1 = C_2 = 22\ \text{nF}$$

Every amplification stage is followed by a second-order Sallen–Key LPF as shown in Figure 7.22. Expression for the corner frequency and high frequency gain are same as that in equation (11.10). Two second-order LPFs are placed before and after the second amplification in Figure 11.10. For better operation, fourth-order LPFs can be used. It needs to be mentioned that

https://doi.org/10.1017/9781108762632.012 Published online by Cambridge University Press

selection of corner frequency depends on the sampling rate that is important in EMG signal acquisition.

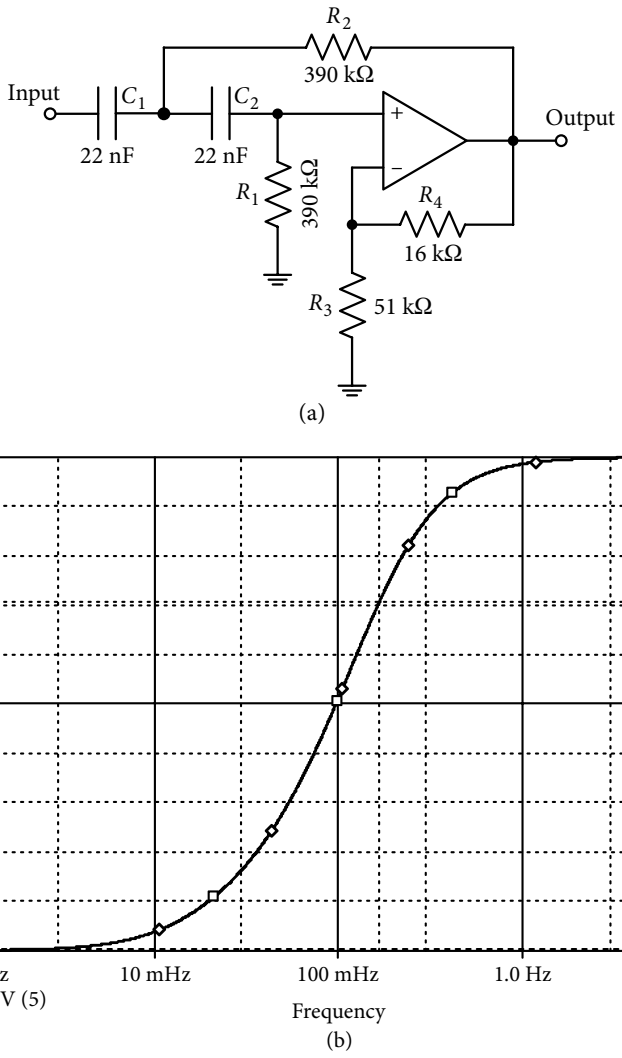

Figure 11.11 (a) Second-order Sallen–Key high pass filter for a 3 dB frequency of 20 Hz. {With permission from Wang et al. [11.17]}. (b) Magnitude response of the high pass filter shown in Figure 11.11(a).

Figure 11.12 shows the simulated responses of the second-order HPF with $f_c = 20$ Hz, fourth-order HPF with $f_c = 20$ Hz, second-order LPF with $f_c = 700$ Hz and $f_c = 1400$ Hz, fourth-order LPF with $f_c = 700$ Hz and $f_c = 1400$ Hz employed in this case study.

A similar study has been done in a conference publication [11.18].

Element values for the second-order LPF, for cut-off frequency of 709 Hz, are as follows:

$R_1 = 68$ kΩ, $R_2 = 68$ kΩ, $R_3 = 51$ kΩ, $R_4 = 24$ kΩ, $C_1 = 3.3$ nF, $C_2 = 3.3$ nF.

https://doi.org/10.1017/9781108762632.012 Published online by Cambridge University Press

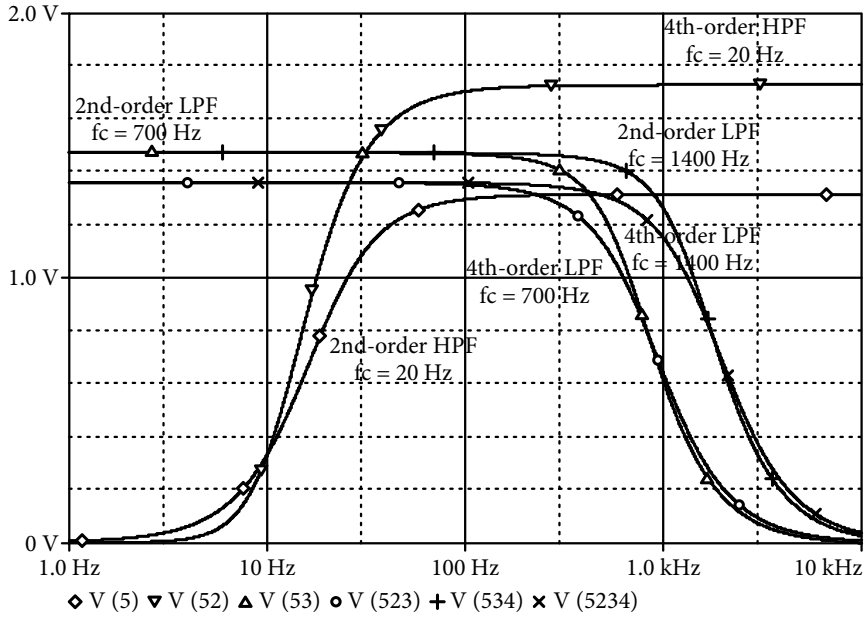

Figure 11.12 Simulated responses of second-order high pass, fourth-order high pass, second-order low pass and fourth-order low pass filters for surface EMG signals.

11.7 Brain–Computer Interface Application

Electroencephalography (EEG) signals are commonly known for the waves representing the electrical activities of the brain. There are five major brain waves depending on the location of where the electrodes are placed. The five signals are different from each other on the basis of their frequency. In spite of the different frequency ranges of these wave types, all the relevant information is confined in the range 1–100 Hz.

Recently, the concept of controlling machines through brain activity, and not just by manual operation, has attracted attention. Being an interdisciplinary concept, researchers in the field of computer science, neuroscience and bio-engineering have joined to develop the prototype of a brain–computer interface (BCI) [11.19].

In general, systems used for the acquisition of EEG signals are similar in nature. However, there are differences on the basis of use of number of electrodes, degree of noise elimination by limiting signals to only the useful frequency range and amount of required amplification. The signals are then digitized and sent to an appropriate output device. Output signals can be used either for diagnostic purposes or other applications such as the BCI application. One of the objectives of developing BCI is to provide a communication channel for users who have lost their ability to communicate normally [11.20].

As mentioned earlier, differences in the practical EEG signal acquisition and the processing system depend on their process of detection and number of channels. However, significant

https://doi.org/10.1017/9781108762632.012 Published online by Cambridge University Press

difference also occurs due to differences in the technological advances in the tools used in signal processing and the required specification of the system itself. In one such example, an attempt was made to show the design of a battery-operated portable single-channel EEG signal acquisition system [11.21].

Magnitude of the EEG signals is in the range 5-500 μV. The signals are fed to an INA 128P inst-amp. Selection of the inst-amp is based on its suitability for battery-operated medical instrumentation having high CMRR, low offset voltage and low drift. A third-order Butterworth active HPF is used to eliminate those noise components which lie below 1 Hz. This kind of filter is shown in Figure 11.13(a). Element values shown in the figure realize a cut-off frequency of 1.0 Hz as given by relation $f_c = 1/2\pi RC$. Its simulated response is shown in Figure 11.13(b).

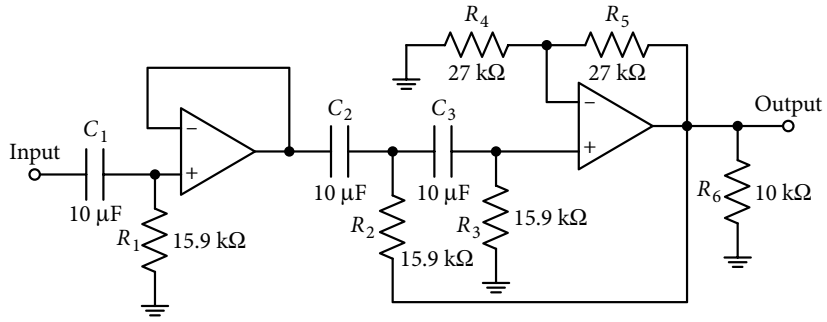

(a)

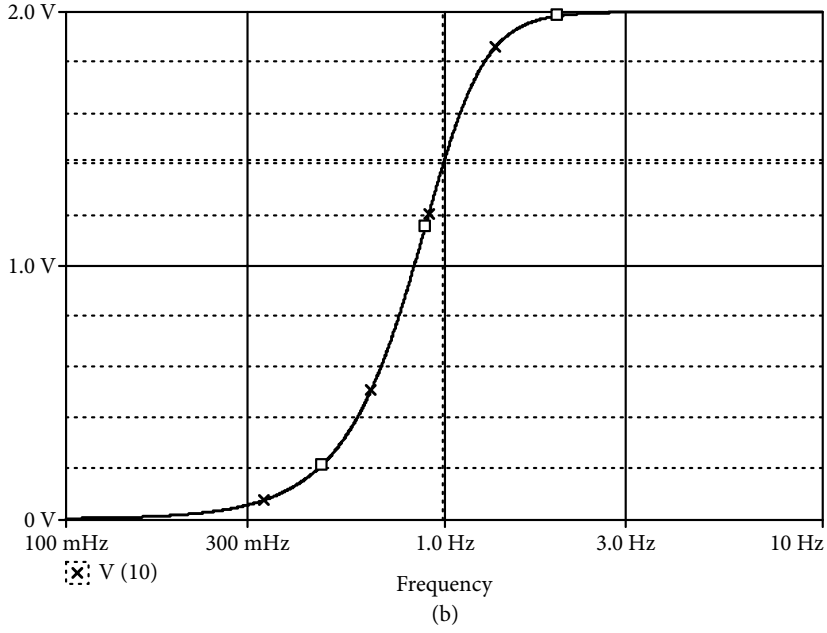

(b)

Figure 11.13 (a) Third-order high pass Butterworth filter for brain–computer interface. {With permission from Bhagwati and Chutia [11.21]} (b) Response of the high pass filter shown in Figure 11.13(a).

https://doi.org/10.1017/9781108762632.012 Published online by Cambridge University Press

The next stage is a third-order Butterworth LPF with a 3-dB frequency of 100 Hz to attenuate noise signals above 100 Hz. Figure 11.14(a) shows the LPF with element values; Figure 11.14(b) shows its simulated response, along with that of the HPF.

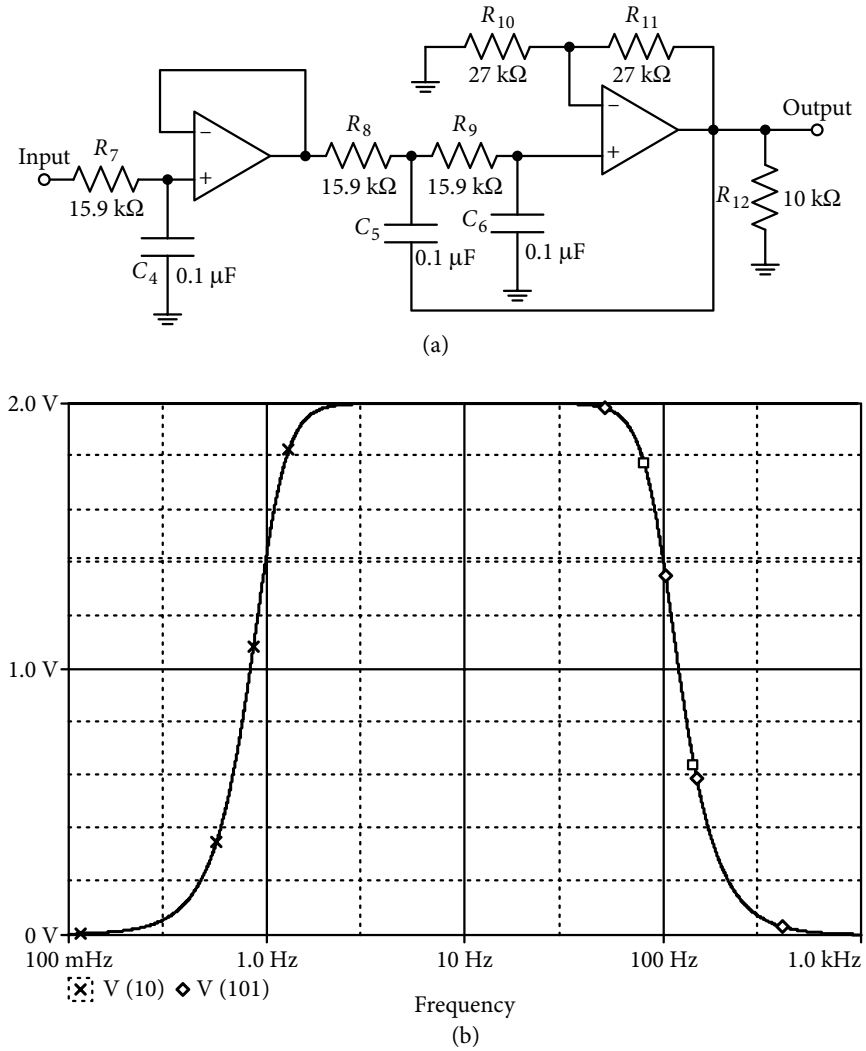

Figure 11.14 (a) Third-order low pass Butterworth filter used to attenuate signals above 100 Hz. (b) Responses of the low pass filter shown in Figure 11.14(a) and the high pass filter shown in Figure 11.13(a).

In addition to the HPF and LPF, it is essential to remove interference of 50/60 Hz due to leakage from the power supply. Conventional twin-tee circuit structure, the one shown in Figure 11.8(a), can be used and does not need any further consideration.

https://doi.org/10.1017/9781108762632.012 Published online by Cambridge University Press

11.8 Chamber Plethysmography

Chamber plethysmography is used to accurately measure absolute changes in blood volume at the extremities, such as finger tips or ear lobes. The blood volume can be converted into blood flow rate. However, when only the pulse rate of the heart is to be found, only information about the relative volume is needed; the amplitude or shape of the signal is not required. In such a case, impedance plethysmography or photo-plethysmography (PPG) can be used [11.22].

In the present case study, PPG sensors have been used in transmission mode on an ear [11.23]. Light transmitted through the aural pinna is detected by a photo sensor. After the first step of optical detection, pulse filtering is done by a second-order BPF with the characteristic frequencies between 1.54 Hz and 2.34 Hz (3 dB frequencies need to be 1.0 Hz and 3.5 Hz) with a gain of 3700 at the peak. It is to be noted that there is specific reason behind selection of the mentioned frequency as it corresponds to wavelength near infrared, and the selected signals have strongest modulation due to the light absorption by the haemoglobin in the blood [11.23].

The circuit topology, shown in Figure 11.15, for realizing the BP characteristic consists of a passive first-order HPF and an active first-order LPF. The transfer function of the BPF is as follows:

$$H(s)=\frac{R_1+R_2}{R_1}\frac{sC_0R_0}{1+sC_0R_0}\frac{1+s\dfrac{R_1R_2}{R_{1+}R_2}C_2}{1+sC_2R_2} \tag{11.11}$$

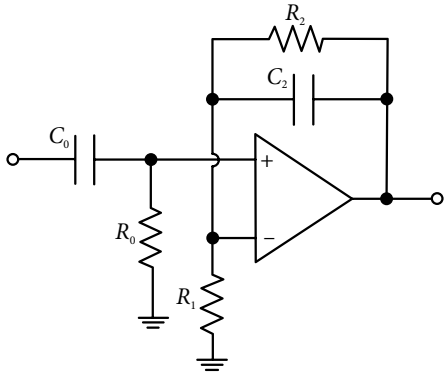

Figure 11.15 Combination of passive high pass and active low pass to realize a band pass function for chamber plethysmograph signal.

Critical frequencies of the LPF and HPF were so selected that the BPF peaks at 2 Hz. To increase the order of the filter, the structure shown in Figure 11.15 was implemented twice and a potentiometer (10 kΩ) was placed in between the two stages to vary the signal gain. Element

https://doi.org/10.1017/9781108762632.012 Published online by Cambridge University Press

values for the filter in Figure 11.15 are: $R_0 = 47$ kΩ, $C_0 = 2.2$ μF, $R_1 = 10$ kΩ, $R_2 = 1000$ kΩ, and $C_2 = 68$ nF. The complete circuit is shown in Figure 11.16(a).

PSpice simulated response of the BPF is show in Figure 11.16(b). Using op amp 741, a peak gain of 3300 (though theoretical value is 10200) occurs at 1.896 Hz while potentiometer branches were 1 kΩ and 9 kΩ.

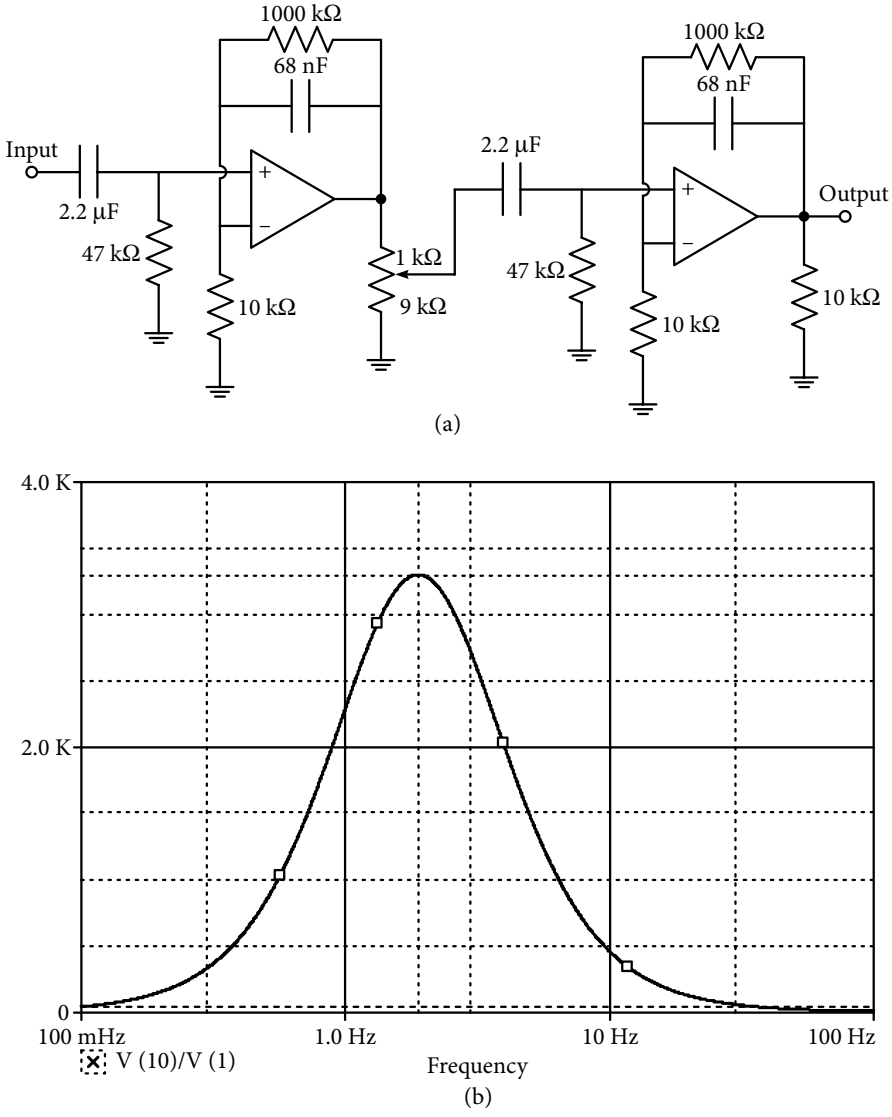

Figure 11.16 (a) A cascade of two sections shown in Figure 11.15 connected through a potentiometer. (b) Simulated response of the fourth-order band pass filter shown in Figure 11.16(a).

https://doi.org/10.1017/9781108762632.012 Published online by Cambridge University Press

11.9 C-Message Weighting Function

A C-message weighting function simulates the frequency response of a human ear. It is a commonly specified test and a measurement filter for voice, audio and telecommunication applications in the US. C-message and similar filters are conventionally fabricated using a cascade of three BPFs and one LPF. The overall characteristics of the C-message filter depend on the parameters of the individual sections. A C-message filter specified by the IEEE standard 743-1984 is an all-pole filter having section parameters as shown in Table 11.1 [11.24].

Table 11.1 Parameters of the second-order sections of a C-message filter

Filter type	Pole values	Critical frequency (Hz)	Pole-Q
BP#1	$-1502\pm j1267$	312.741	0.6540
BP#2	$-2437\pm j5336$	933.761	1.2027
BP#3	$-4690\pm j15267$	2541.886	1.7026
LP#1	$-4017\pm j21575$	3492.728	2.7316

In actual practice, individual sections are fabricated with digitally programmable center frequency and pole-Q. Maxim Integrated in its application note 11 has realized such a C-message filter using switched capacitors. However, current examples have shown the same response with continuous-time second-order sections. For practical applications, these filters can also be made programmable.

The circuit shown in Figure 7.7 was used for the realization of the three BPFs, and the circuit shown in Figure 7.6 was used for the realization of LPF. It gives the following element values for the second-order sections.

BP#1 $R_1 = 49.28$ kΩ, $R_2 = 184$ kΩ, $R_3 = 66.6$ kΩ, $C_3 = 10$ nF, $C_5 = 10$ nF

BP#2 $R_1 = 16.01$ kΩ, $R_2 = 12.3$ kΩ, $R_3 = 40.9$ kΩ, $C_3 = 10$ nF, $C_5 = 10$ nF

BP#3 $R_1 = 2.82$ kΩ, $R_2 = 5.28$ kΩ, $R_3 = 21.3$ kΩ, $C_3 = 10$ nF, $C_5 = 10$ nF

LP#1 $R_1 = 5.4$ kΩ, $R_3 = 10$ kΩ, $R_4 = 10$ kΩ, $C_2 = 49.7$ nF, $C_5 = 0.4168$ nF

It needs to be mentioned that the voltage gain of the respective filter sections, as suggested in the application note 11 of Maxim Integrated is taken as 0.675, 0.685, 0.864, and 2.0, respectively. The overall eighth-order filter is shown in Figure 11.17(a) and its simulated response is shown in Figure 11.17(b) which matches with standard C-message.

https://doi.org/10.1017/9781108762632.012 Published online by Cambridge University Press

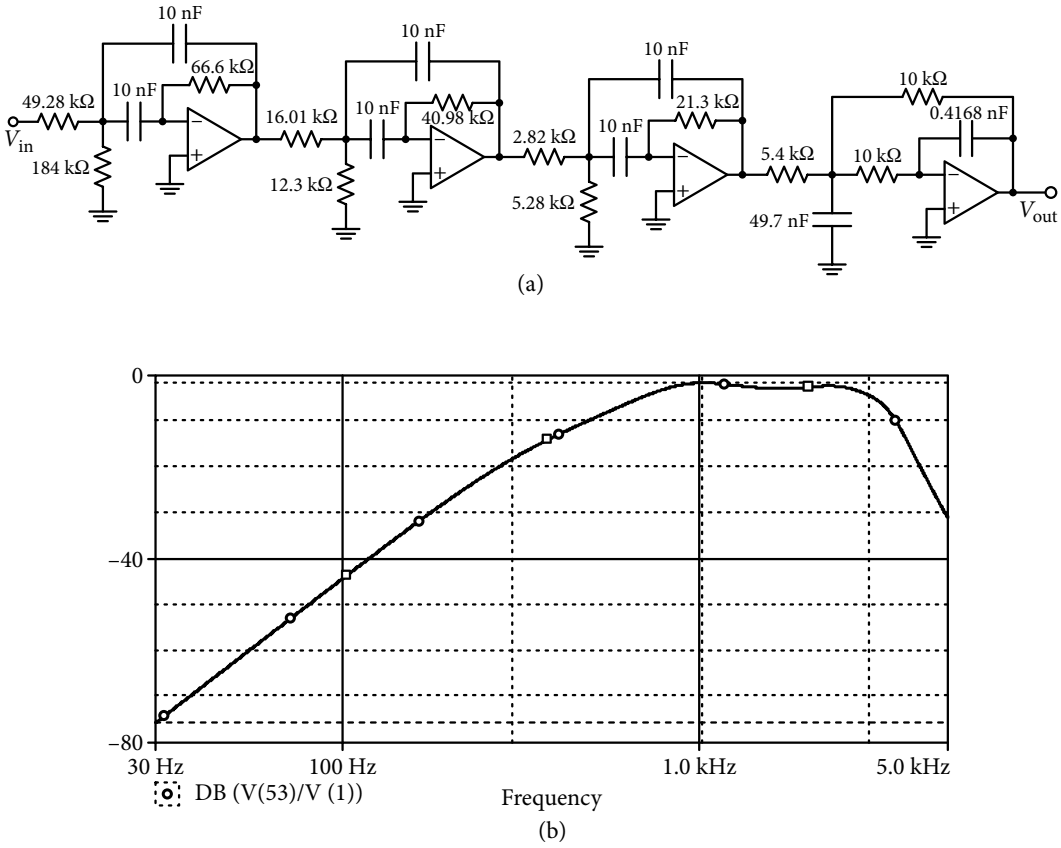

Figure 11.17 (a) Cascade of three band pass filters and a low pass filter for generating a C-message weighting function. (b) Simulated C-message weighting function for the circuit shown in Figure 11.17(a).

References

[11.1] Prutchi, David and Michael Norris. 2005. *Design and Development of Electronic Instrumentation*. New Jersey: Wiley Interscience, John Wiley and Sons Inc., Publication.

[11.2] Kitchin, Charles and Lew Counts. 2006. 'Monolithic Instrumentation Amplifier.' Chapter II and III A in *Designer's Guide to Instrumentation Amplifiers*. US: Analog Devices.

[11.3] 'USBPGF-S1. USB Programmable Single Channel Instrumentation Amplifier and Low Pass Filter'. Costa Mesa, CA, US: Alligator Technologies. https://alligatortech.com/downloads/USBPGF-S1_Data_Sheet.pdf.

[11.4] Texas Instruments. 2019. *Low Power Instrumentation Amplifier INA 102 Data Sheet*. SBOSO27B. US: Burr Brown Corporation.

[11.5] Larsen, Cory. A. 2010. *Signal Conditioning Circuitry Design for Instrumentation System*. SAND2011-9467. Cal. US: Sandia National Laboratories.

https://doi.org/10.1017/9781108762632.012 Published online by Cambridge University Press

[11.6] Walters, P. L. 2010. *Measurement System Engineering*. Short Course at Sandia National Laboratory. Cal. US: Sandia National Laboratories.

[11.7] Reyerson, D. E. 1996. *Signal Conditioning Primer*. Cal. US: Sandia National Laboratories.

[11.8] Texas Instruments. 2011. *Filter Pro Users' Guide*.

[11.9] Texas Instruments. P O Box 655303, Dallas, Texas 75265 USA. Linear Technology Corporation 1630 McCarthy Blvd, Milpitas, C 95035-7417 (www.linear.com), Maxim Electronics Products and Analog Devices (www.maximintegrated.com/conact). ON Semiconductors P O Box 61312, Phoenix, Arizona85082-1312 USA. (http://onsemi.com). Microchip Technology Incorporated, 2355 West Chandler Blvd, Chandler AZ 85224-6199.

[11.10] Maxim Integrated Products. 2010. *Introduction to Electrocardiographs*, Tutorial 4693. US: Maxim Integrated Products, Inc.

[11.11] Lee, Shuenn-Yuh, Jia-Hua Hong, Jin-Ching Lee, and Qiang Fang. 2012. 'An Analog Front-End System with a Low-Power On-Chip Filter and ADC for Portable ECG Detection Devices.' In *Advances in Electro-Cardiogram-Methods and Analysis*, edited by Richard Miller., Germany: IntechOpen.

[11.12] Webster, G. J. 1995. *Design of Cardiac Pace Maker*. NJ: IEEE Press.

[11.13] Lasanen, K., and J. Lostamovaara. 2005. 'A 1V Analog Front-end for Detecting QRS Complexes in a Cardiac Signal,' *IEEE Transactions on Circuit Systems* 42 (10): 2161–8.

[11.14] Salthouse, C. D., and R. Sarpeshkar. 2003. 'A Practical Micropower Programmable Band Pass Filter used in Bionic Ears,' *IEEE Journal of Solid-State Circuits* 38 (1): 63–70.

[11.15] Solís-Bustos, Sergio, José Silva-Martínez, Franco Maloberti, and Edgar Sánchez-Sinencio. 2000. 'A 60-dB Dynamic Range CMOS Sixth-Order 2.4-Hz Low Pass Filter for Medical Applications,' *IEEE Transactions on Circuit and Systems-II, Analog and Digital Signal Processing* 47 (12): 1391–8.

[11.16] Wang, Kening, Shengqian Ma, Jing Feng, Weizhao Zhang, Manhong Fan, and Dan Zhao. 2012. 'Design of ECG Signal Acquisition System Based on DSP'. *SciVerse Science Direct, Procedia Engineering* 29: 3763–7.

[11.17] Wang, S., L. Tang, and J. E. Bronlund. 2013. 'Surface EMG Signal Amplification and Filtering,' *International Journal of Computer Applications* 82 (1): 0975–8887.

[11.18] Shobaki, Mohammed M., Noreha Abdul Malik, Sheroz Khan, Anis Nurashikin, Samnan Haider, Sofiane Larbani, Atika Arshad, and Rumana Tasnim. 2013. 'High Quality Acquisition of Surface Electromyography: Conditioning Circuit Design,' *IOP Conference Series: Material Science and Engineering* 53: 12027.

[11.19] Rani, M. S. A., and Wahida B Mansor. 2009. 'Detection of Eye Blinks from EEG Signals for Home Lighting Systems,' *Proc. ISMA09.* Sharjah, UAE: International Symposium on Mechatronics and Its Applications.

[11.20] Wolpaw, Jonathan R., Niels Birbaumer, William J. Heetderks, Dennis J. McFarland, P. Hunter Peckham, Gerwin Schalk, Emanuel Donchin, Louis A. Quatrano, Charles J. Robinson, and Theresa M. Vaughan. 2000. 'Brain-Computer Interface Technology: A Review of First International Meeting,' *IEEE Transactions on Rehabilitation Engineering* 8 (2): 164–173.

[11.21] Bhagwati, A. J., and R. Chutia. 2016. 'Design of Single Channel Portable EEG Signal Acquisition System for Brain Computer Interface Application,' *International Journal of Biomedical Engineering and Science* 3 (1): 37–44.

[11.22] Webster, John. G. (ed.). 1992. *Medical Instrumentation, Applications and Design*, second edition. Mass, US: Houghton Mifflin Co.

[11.23] Langereis, Geert. 2010. *Photo-plethysmography (PPG) System*, Version 2 (www.semanticscholar.org).

[11.24] Maxim Integrated. 1998. 'Programmable Universal Filter Implements C-Message Weighting Function,' Application Note 11. US: Maxim Integrated.

Practice Problems

11-1 Laplace representation is used for a three-level system of fluorescent spectroscopy by a simple cascade of filters as shown in Figure 2.7(b). Let life-time for fast relaxation be 10^{12} seconds and life-time for the slow relaxation is $0.5*10^4$ seconds life-time of the first-stage LPF for both the cases was set at 1.1 second. Design the filters and find the phase shift for the two sets at 10 kHz and 100 kHz.

11-2 Equivalent circuit for the transfer function with two life-time components is shown in Figure 2.8(a). Signal frequencies used for the slow and the fast transition rates in the circuit were 1 krad/s and 1 Mrad/s. Design the two filter sections and add their outputs while changing the weightage of the output of the slow transition state. What will be the phase shift at 1 kHz when the weightage of the slow state with respect to the fast state transition is 1, 0.75, 0.5 and 0.25.

11-3 Design an instrumentation amplifier using 741 type operational amplifiers (BW = $2\pi*10^6$ rad/s) as shown in Figure 11.3. Voltage gain value will be 1, 2, 5, 10, and 20 by varying a single resistance. Assume suitable values for the resistances and find the bandwidth of the instrumentation amplifier as a function of the gain value.

11-4 Instrumentation amplifier AD8224B is to be used to obtain an LPF for the following specifications. Output voltage should become 1 volt at dc for a differential input signal of 25 mV, and its 3-dB frequency is to be 25 kHz. Design and test the circuit.

11-5 Input to an 8-bit ADC working on sampling frequency of 100 kHz, receives non-aliased signal up to 30 kHz. The voltage level at the input of the ADC is to be 4 volts. Design a maximally flat LPF that provides sufficient attenuation for the proper working. The ADC employed the instrumentation amplifier to band limit the input signal and acted as a pre-amplifier with gain of 10. Input to the instrumentation amplifier was at an amplitude of 25 mV.

11-6 With other specifications remaining the same, repeat problem 11-5 for a 12-bit ADC.

11-7 Phase compensation is to be used to linearize the phase of the Butterworth response obtained in the problem 11-4. The compensation filter should have less than 10% phase non-linearity aver the pass band. Design analog phase compensating filter utilizing the circuit (or cascade) of Figure 4.6(b).

11-8 Amplitude of an ECG signal was 2 mV, which was pre-amplified by a factor of 100. The signal is to be band-limited up to 250 Hz using a third order Chebyshev approximation with 1 dB ripple such that its output voltage level becomes 1 volt. Design and test the filter.

11-9 Output of the LPF in problem 11-8 is fed to a Sallen–Key HPF structure to minimize low frequency noise. 3-dB frequency of the HPF is to be 0.1 Hz with its gain being 1.5. Design and test the filter.

11-10 Design a notch filter for suppressing the noise frequency of 50 Hz/ 60 Hz on the acquisition board of an 'analog front-end' of an ECG system. Employ the notch filter structure of Figure 8.10(a).

https://doi.org/10.1017/9781108762632.012 Published online by Cambridge University Press

11-11 A BPF is to be designed for an ECG signal acquisition system employing the operational amplifier OPA 2604. The BPF is obtained as a combination of an LPF with cut-off frequency of 500 rad/s and an HPF with cut-off frequency of 0.3 rad/s.

At what frequency the output falls to half of its maximum magnitude?

11-12 Electromyography signal was pre-amplified and fed to an HPF. Design the HPF with gain of 10 using biquad structure of Figure 7.8(a) having 3-dB frequency of 20 Hz.

Cascade two second-order HPFs and re-design the filter with the same specifications.

11-13 An LPF is to be used in the chain of Electromyograph signal processing. Design a second-order filter using Sallen–Key structure and OPA 2604 operational amplifier, with cut-off frequency of 40 krad/s.

11-14 Combine the second-order HPF of problem 11-12 and a second-order LPF of problem 11-13 to yield a BPF. What are frequencies at which the gain falls to half of its mid-band gain?

11-15 ECG signal is to processed through a BPF which is a combination of a maximally flat third-order LPF and a third-order HPF. Both the filters are realized by cascading a first-order and a second-order filter section. In each case the second-order section employs general differential input single OA biquad configuration of Figure 7.13. Respective corner frequencies of the LPF and the HPF are 600 rad/s and 6 rad/s.

What is the frequency range of the pass band of the composite filter?

11-16 Circuit shown in Figure 11.15 is utilized to obtain a second-order BPF. Select component values such that dc gain of the LPF and the high frequency gain of the HPF is 100, and respective corner frequencies are 20 rad/s and 1.6 rad/s.

What is the peak gain of the BPF and at what frequency it occurs?

11-17 Critical frequencies of the filter components of the standard C-message weighting function are increased by 10%, and respective pole-Q are reduced by 5%. Obtain modified response and compare gain values between the two responses at 100 Hz, 1 kHz and 2 kHz.

https://doi.org/10.1017/9781108762632.012 Published online by Cambridge University Press